GMR
The Original

WOUND HEALING POTENTIAL OF MULTISCALE POLYMERIC NANOCOMPOSITE LOADED WITH CuO NANOPARTICLES FROM *Sargassum muticum* EXTRACT ON HaCaT KERATINOCYTE CELLS MODEL

Akshayaa Paramasivan[1], Chakradhar Arepalli[2], Sattanathan Govindharajan[3]*

[1]Saveetha Medical College & Hospital (SMCH), Saveetha Institute of Medical and Technical Sciences (SIMATS), Thandalam, Chennai, Tamil Nadu 602105, India. akshivan1965@gmail.com
[2]Department of Nephrology, Saveetha Medical College and Hospital, Saveetha Institute of Medical And Technical Sciences (SIMATS), Thandalam, Chennai-602105, Tamil Nadu, India. Email: arepalli.chakri@gmail.com
[3]Department of Pathology, Saveetha Medical College and Hospital, Saveetha Institute of Medical And Technical Sciences (SIMATS), Thandalam, Chennai-602105, Tamil Nadu, India. Email: sattanathanphd@gmail.com
*Corresponding Author: sattanathanphd@gmail.com (S.G.)

ABSTRACT

This study investigates the wound healing potential of novel starch/polyvinyl alcohol (PVA) electrospun nanocomposite embedded with biogenically synthesized copper oxide nanoparticles (CuO NPs) derived from *Sargassum muticum* extract. The CuO NPs were synthesized via an ultrasonic-assisted green method and characterized using UV-Vis spectroscopy, Fourier-transform infrared spectroscopy (FTIR), X-ray diffraction (XRD), Scanning electron microscopy (SEM), Thermogravimetric analysis (TGA), and zeta potential analysis. UV-Vis spectroscopy confirmed nanoparticle formation with a distinct SPR peak at 270 nm, while FTIR and XRD verified the presence of functional groups and monoclinic crystalline structure, respectively. SEM revealed well-dispersed CuO NPs within the porous nanofiber scaffold, which exhibited enhanced thermal stability. *In vitro* wound healing assays using HaCaT keratinocytes demonstrated that the starch/PVA/CuO-NPs nanoscaffolds significantly accelerated cell migration, achieving up to 96.14% wound closure at 100 µg/mL—outperforming both algal extract (70.14%) and CuO NPs alone (84.14%). The results highlight the synergistic effect of the biocompatible nanocomposite and bioactive CuO NPs, positioning them as a promising advanced wound dressing material. Further research into their *in vivo* efficacy and mechanistic pathways is warranted.

KEYWORDS: *Sargassum muticum*, Green synthesis, CuO NPs, Starch/PVA- nanocomposite, Wound-healing activity.

1. INTRODUCTION

Wound healing is a complex, multistep biological process that is essential for restoring the structural and functional integrity of damaged tissues [1]. This process involves a cascade of cellular events, including hemostasis, inflammation, proliferation, and remodeling [2]. Despite its natural efficiency, certain clinical conditions such as chronic wounds, diabetic ulcers, and infections often impair the healing process [3]. These complications place a considerable burden on public health systems worldwide, necessitating the development of novel therapeutic strategies that can accelerate and enhance wound repair [4]. Among emerging approaches, nanotechnology-based interventions have garnered significant attention, particularly in the form of bioengineered nanoscaffolds integrated with therapeutic agents [5].

Electrospun nanocomposite have emerged as promising wound dressings due to their high surface area, interconnected porous structure, and excellent biocompatibility, which collectively support cellular adhesion, migration, and proliferation [6]. Polymers like starch and polyvinyl alcohol (PVA) have been widely employed in nanofiber fabrication for biomedical applications [7]. Starch, a natural polysaccharide, is biodegradable, biocompatible, and abundant, while PVA is a synthetic, water-soluble polymer known for its mechanical stability and film-forming ability [8]. Blending these two polymers facilitates the development of hybrid nanoscaffolds that can mimic the native extracellular matrix (ECM), thereby enhancing tissue regeneration [9].

Incorporating nanoparticles into polymeric nanocomposite has further expanded the scope of wound healing applications [10]. Among various metal oxide nanoparticles, copper oxide nanoparticles (CuO NPs) have shown remarkable potential due to their intrinsic antimicrobial, anti-inflammatory, and angiogenic properties [11]. Copper ions play a critical role in various physiological processes, including collagen formation, vascular endothelial growth, and stabilization of the ECM [12]. The integration of CuO NPs into electrospun scaffolds not only enhances their biological performance but also imparts antimicrobial protection, which is crucial in preventing wound site infections [13].

Traditionally, chemical and physical methods for nanoparticle synthesis often involve toxic reagents, energy-intensive conditions, and hazardous by-products [14]. In contrast, green synthesis using biological resources offers

an eco-friendly, sustainable, and cost-effective alternative [15]. Marine macroalgae have emerged as promising candidates for the green synthesis of nanoparticles owing to their rich reservoir of bioactive compounds such as polyphenols, flavonoids, proteins, and polysaccharides, which act as natural reducing and stabilizing agents [16]. Among brown algae, *Sargassum muticum* is particularly notable for its high content of biofunctional molecules and therapeutic potential [17]. Its widespread availability along coastal regions, including the Indian coastline, makes it an ideal source for eco-conscious nanoparticle synthesis [18].

Ultrasonic-assisted extraction techniques have further improved the efficiency of bioactive compound retrieval from algal biomass [19]. The application of ultrasound facilitates cavitation, enhancing cell wall disruption and improving the yield of phytochemicals [20]. These extracts, when utilized in nanoparticle synthesis, result in uniform, stable nanoparticles with improved biological functionalities [21]. The resulting biogenic CuO NPs exhibit desirable properties for incorporation into wound-healing scaffolds [22].

In this study, we present the development and evaluation of a novel starch/PVA electrospun nanofibrous scaffold incorporated with green-synthesized CuO NPs using *S. muticum* extract [23]. The macroalga was harvested from the intertidal zones near Rameswaram, a region rich in marine biodiversity [24]. The algal extract was prepared using ultrasonic-assisted extraction to ensure the efficient release of phytoconstituents responsible for nanoparticle formation [25]. The green synthesis of CuO NPs was monitored and confirmed through a visible color change and characterized using a suite of analytical techniques, including UV–Vis spectroscopy, Fourier-transform infrared spectroscopy (FTIR), X-ray diffraction (XRD), Scanning electron microscopy (SEM), Thermogravimetric analysis (TGA), and zeta potential analysis [26].

The biogenic CuO NPs were blended into a starch/PVA matrix, and nanofibers were fabricated via electrospinning under optimized parameters to obtain uniform, continuous fibers [27]. These nanofibrous mats were further evaluated for their physicochemical properties and biological activity [28]. Particular emphasis was placed on assessing their wound healing efficacy using an *in vitro* scratch assay on HaCaT keratinocyte cells [29]. This assay mimics the process of cell migration during wound closure and provides insight into the therapeutic effectiveness of the test materials [30].

The integration of green-synthesized CuO NPs into a biodegradable polymer matrix represents a significant advancement in wound care technology [31]. The synergy between the polymeric scaffold and metal oxide nanoparticles is anticipated to improve cell proliferation, promote re-epithelialization, and enhance overall healing rates [32]. Furthermore, the environmentally friendly synthesis route underscores the sustainability aspect of this biomedical material [33].

Overall, the present work bridges marine biochemistry, nanotechnology, and tissue engineering to propose a sustainable and efficient strategy for wound healing applications. The utilization of *S. muticum* not only valorizes marine biomass but also demonstrates its practical applicability in the synthesis of functional nanomaterials. Through detailed physicochemical characterization and biological evaluation, this study lays the groundwork for future translational research aimed at developing clinically viable wound dressing systems.

2. MATERIALS AND METHODS

2.1. Collection and processing of marine macroalgae

S. muticum specimens were hand-harvested from intertidal coastal areas near Rameswaram. The collected *Sargassum muticum* was taxonomically identified and authenticated by Dr V. Veeragurunathan, CSIR-CSMCRI-Marine Algal Research Station, Mandapam Camp 623519, Tamil Nadu, India. A voucher specimen was prepared and deposited at the Herbarium of the CSIR-CSMCRI-Marine Algal Research Station, under the accession number: SI–2025–RMM–016. This authentication ensures botanical accuracy and standardization of the study material. Post-collection, the samples were immediately placed in chilled containers to preserve their biological integrity during transit to the laboratory. Upon arrival, the seaweed was washed thoroughly under running tap water to eliminate sand, debris, and surface contaminants, including epiphytes. Subsequent rinsing with distilled water ensured further purification. The cleaned macroalgae were then chopped into smaller pieces and dried in a shaded, well-ventilated room at ambient temperature for approximately 14 days. Once fully dried, the biomass was pulverized into a fine powder using a mechanical milling device and stored in sealed containers at room temperature for future procedures.

2.2. Ultrasonic extraction of phytocompounds

To extract bioactive constituents, 2 grams of powdered *S. muticum* were mixed with 50 mL of Milli-Q-grade water. This suspension underwent ultrasonic extraction using a LABQUEST ultrasonic bath (Borosil; Serial No. 941032329018) set at 60°C for 45 minutes. The ultrasound-assisted method facilitated the breakdown of cell walls and enhanced compound release. Following sonication, the mixture was filtered using sterile Whatman No. 1 filter paper to obtain a clean extract. The resulting solution was stored temporarily at 10°C and subsequently freeze-dried via lyophilization for prolonged storage and downstream experimental use [34, 35].

2.3. Green fabrication of CuO NPs

CuO NPs were synthesized using a green route by combining 50 mL of a 0.1 M aqueous $CuSO_4 \cdot 5H_2O$ solution with 10 mL of *S. muticum* extract, which was prepared by dissolving 10 mg of lyophilized extract in 10 mL Milli-Q water (5:1 volume ratio). The resulting mixture was stirred at a constant speed of 650 rpm and heated at 60°C

for a duration of 2 hours. The reaction progress was visually indicated by a color change from blue to bluish-green, suggesting the reduction of copper ions and CuO formation. The reaction mixture was centrifuged, and the pellet was washed thrice with double-distilled water to eliminate impurities and organic residues. The purified nanoparticles were lyophilized for 48 hours and preserved in airtight containers for later characterization and scaffold development [36].

2.4. Electrospinning of starch/PVA nanofibers embedded with CuO NPs

To develop composite nanofibers, a 15% (w/w) PVA solution was prepared by dissolving the polymer in Milli-Q water under continuous stirring. Subsequently, 100 mg each of starch and synthesized CuO NPs were incorporated into the PVA solution. The mixture was stirred thoroughly at 50°C for 2.5 hours to ensure homogeneous dispersion of the components. This blended solution was loaded into a syringe with a stainless-steel nozzle (0.84 mm internal diameter) and mounted on the HOLMARC HO-NFES-040 electrospinning unit. Optimized electrospinning parameters included an applied voltage of 11.5 kV, a needle-to-collector distance of 12.3 cm, and a flow rate of 0.4 mL/h. The process was conducted at ambient conditions for 6–8 hours, after which the nanofibrous mats were collected and stored in a desiccator for subsequent evaluations [37-39].

2.5. Physicochemical characterization of nanoparticles and nanofiber mats

2.5.1. UV–visible spectroscopy

The optical characteristics of both the *S. muticum* extract and the synthesized CuO NPs were determined using a VIS SPEC V-730 spectrophotometer. Measurements were recorded across a wavelength range of 200 to 800 nm, using deionized water as the blank reference. The emergence of surface plasmon resonance (SPR) peaks confirmed successful nanoparticle synthesis [40].

2.5.2. FTIR spectroscopy analysis

FTIR spectra were acquired using a PerkinElmer Spectrum Two instrument in ATR mode. Spectral data were collected between 4000 and 400 cm^{-1}, with a resolution of 4 cm^{-1} and 64 scans per sample. Peaks were interpreted based on functional groups including hydroxyl, phenol, carbonyl, and metal-oxygen bonds to determine chemical interactions and nanoparticle composition [41].

2.5.3. XRD analysis

XRD analysis was carried out using a Bruker D8 Advance diffractometer equipped with CuKα radiation (λ = 1.5406 Å), operating at 40 kV and 40 mA. Diffraction patterns were captured over a 2θ range of 5°–90° with a step size of 0.029649°. The observed diffraction peaks were matched with standard JCPDS files to validate the crystalline structure and phase purity of CuO NPs [42].

2.5.4. SEM analysis

Surface topography and dispersion of nanoparticles within the electrospun fibers were analyzed using a JEOL JSM-IT800 NANO SEM. Prior to imaging, samples were gold-sputtered to improve conductivity. SEM images provided insight into fiber diameter, surface texture, and distribution uniformity of embedded nanoparticles [43].

2.5.5. TGA

The thermal behavior of the composite nanofiber mats was evaluated using a PerkinElmer TGA 8000 instrument. Roughly 5 mg of each sample was heated from room temperature up to 550°C at a rate of 15°C/min under a nitrogen atmosphere. The resulting thermograms were interpreted for moisture loss, polymer decomposition, and residual content [44].

2.5.6. Particle size and zeta potential determination

The average particle size and surface charge of the synthesized CuO NPs were measured with a Malvern Zetasizer Ultra. The zeta potential values were assessed to estimate colloidal stability, with higher absolute values indicating better electrostatic repulsion and dispersion quality [45].

All generated data from these experiments have been deposited in the Mendeley Data repository, accessible via DOI: 10.17632/jrs2y2hp7v.2.

2.6. Wound healing (scratch) assay

The *in vitro* scratch assay was employed to assess the cell migration potential of HaCaT keratinocytes upon treatment with different formulations: *S. muticum* extract, CuO NPs, and starch/PVA/CuO-NPs nanoscaffolds. Cells were seeded in 12-well plates at a density of 2×10^5 cells/well using Dulbecco's Modified Eagle Medium (DMEM) supplemented with 10% FBS and 1% penicillin–streptomycin. After reaching confluence in a 5% CO_2 incubator at 37 °C, a linear wound was created using a sterile 200 µL pipette tip. Detached cells were removed with PBS, and treatment solutions (6.25, 12.5, 25, 50, and 100 µg/mL) were added in serum-free DMEM. Untreated wells acted as controls. Images were captured at 0, 24, and 48 hours using an inverted phase-contrast microscope, and wound closure rates were calculated using ImageJ to compare treatment effectiveness [46].

2.7. Statistical analysis

All experimental results were analyzed statistically using SPSS v25.0 and GraphPad Prism v9.0. Data are expressed as mean ± standard deviation from triplicate tests. Differences among groups were determined by one-way ANOVA followed by Tukey's or Dunnett's post hoc test. A significance level of $p < 0.05$ was adopted. Pearson correlation tested inter-variable associations. Data normality was verified via the Shapiro–Wilk test, and

log transformation was applied if normality assumptions failed. A 95% confidence level was maintained for all interpretations [47].

3. RESULTS

3.1. UV–visible spectroscopy

The optical absorbance profiles of *S. muticum* extract and the green-synthesized CuO NPs were recorded using a JASCO V-730 UV–Vis spectrophotometer across a spectral range of 200–800 nm with a resolution increment of 1 nm (Fig. 1). The crude algal extract displayed a broad absorption band characteristic of its diverse phytochemical constituents. In contrast, the CuO NPs exhibited a marked SPR peak centered at 270 nm, which serves as a spectral fingerprint confirming nanoparticle formation. The absorbance intensity at this peak measured 0.4776, indicating the presence of nanoscale copper oxide structures. The instrumental parameters, including a 1.0 nm slit width, a scanning rate of 1000 nm/min, and automated filter switching, enabled precise spectral acquisition. This distinct optical behavior validated the transformation of copper salts into nanosized CuO particles via biogenic synthesis.

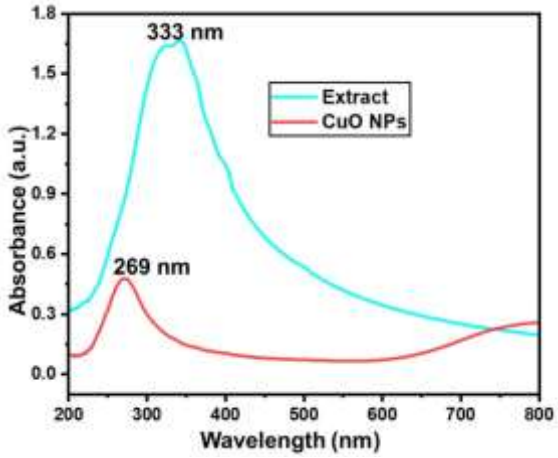

Fig. 1. UV–Visible spectral profiles of algal extract and CuO NPs.

3.2. FTIR spectroscopy

Attenuated total reflectance Fourier-transform infrared (ATR-FTIR) spectra were captured using a PerkinElmer Spectrum Two spectrophotometer to investigate the functional groups present in the CuO NPs and the starch/PVA electrospun matrix (Fig. 2). The CuO NPs revealed a broad absorption peak at 3277 cm^{-1}, corresponding to O–H stretching vibrations, alongside minor peaks near 2700 and 2500 cm^{-1}, which may signify C–H stretching or aldehydic carbonyl functionalities. The starch/PVA nanoscaffold demonstrated a strong C=O stretching vibration at 1500 cm^{-1}, while the peak around 840 cm^{-1} was attributed to glycosidic linkages inherent to starch. Peaks observed below 1000 cm^{-1}, especially near 600 cm^{-1}, were indicative of Cu–O bonding, confirming the incorporation of copper oxide particles into the polymeric matrix. These spectral features confirmed that essential molecular structures were retained and that CuO NPs were effectively embedded into the nanofiber scaffolds.

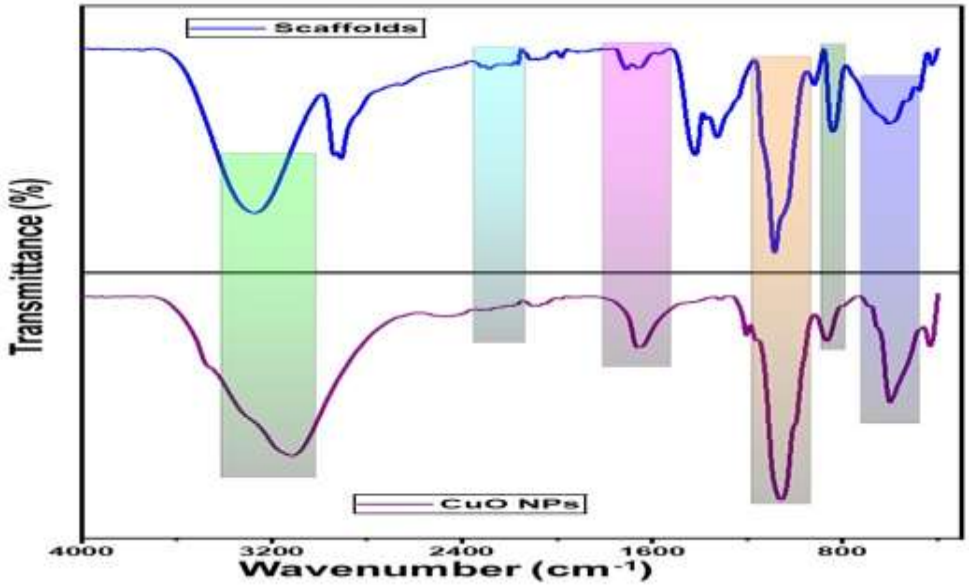

Fig. 2. FTIR spectra of CuO NPs and their incorporation into nanoscaffolds.

3.3. XRD analysis

XRD analysis was performed using a Bruker D8 Advance diffractometer equipped with CuKα radiation (λ = 1.5406 Å), scanning over a 2θ range from 5° to 90°. The CuO NPs exhibited prominent peaks at 32.7° (110), 35.3° (002), 38.3° (111), and 48.1° (202), which match the diffraction pattern for a monoclinic phase of CuO, corroborated by JCPDS card no. 05-0661. The electrospun starch/PVA scaffold revealed semicrystalline peaks at 19.3°, 21.4°, and 23.5°, supplemented by additional reflections at 26.5° and 29.5° (Fig. 3), suggesting structural alteration due to nanoparticle inclusion. Calculated interplanar spacings were 2.73 Å for the CuO NPs and 4.60 Å for the scaffold composite, reinforcing the crystalline nature of the nanoparticles and their even distribution within the polymer framework.

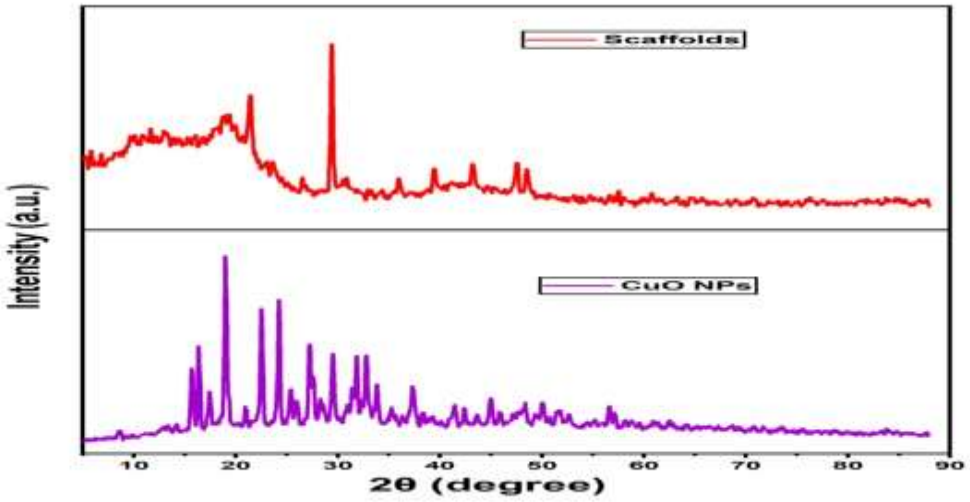

Fig. 3. XRD patterns of synthesized CuO NPs and CuO-loaded scaffolds.

3.4. SEM analysis

Morphological characteristics of the synthesized CuO NPs and starch/PVA nanoscaffolds were examined through SEM using a JEOL JSM-IT800 NANO microscope (Fig. 4). The CuO NPs appeared as aggregates with varying morphologies ranging from spherical to irregular, suggesting polydispersity. In contrast, the starch/PVA nanofibers displayed a well-defined porous and fibrous structure with relatively smooth surfaces and minor bead formation, which are typical in electrospun mats. The nanoparticles were visibly integrated and dispersed throughout the nanofiber surface, confirming their successful entrapment. The microstructural arrangement indicated that the scaffold offers an advantageous architecture for biomedical applications involving tissue support and cell migration.

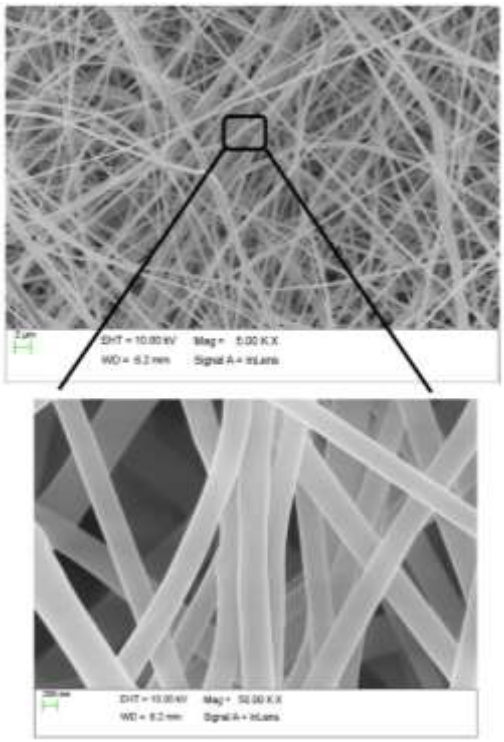

Fig. 4. SEM analysis of synthesized CuO NPs and CuO-loaded scaffolds.

3.5. TGA

Thermal stability of the nanocomposite scaffolds was evaluated through TGA conducted under a nitrogen atmosphere from 25°C to 550°C (Fig. 5). The thermogram indicated a three-step degradation profile. The initial mass loss occurred below 150°C, attributed to moisture evaporation. The second phase began at approximately 243.0°C and peaked at 349.6°C, corresponding to the thermal decomposition of starch and PVA. The final residual mass was approximately 51.9%, suggesting the presence of thermally resistant inorganic components and possible crosslinking. These results confirmed that the inclusion of CuO NPs enhanced the scaffold's thermal stability and that the scaffold maintained its structural coherence up to the onset of major degradation.

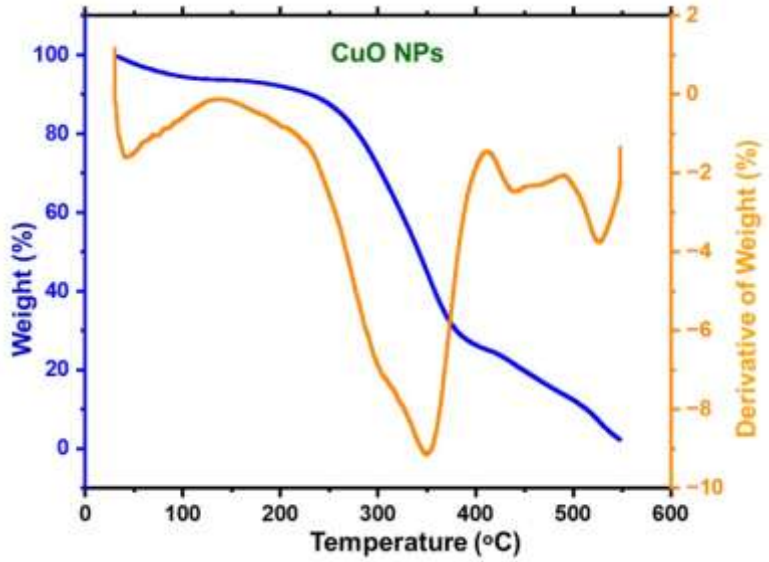

Fig. 5. Thermal degradation behavior of CuO-incorporated nanoscaffolds.

3.6. Zeta potential and particle size analysis

Dynamic light scattering (DLS) measurements showed that the biosynthesized CuO NPs had a hydrodynamic diameter of 92.1 nm and a polydispersity index (PDI) of 0.8444, indicating a moderately broad particle size distribution (Fig. 6). Zeta potential analysis revealed a surface charge of −12.62 mV, with peak values recorded at −20.85 mV and −8.99 mV (Fig. 7), indicating that the colloidal system has moderate electrostatic stability due to surface charge repulsion. The measured conductivity of the solution was 0.07909 mS/cm, and the quality factor was 5.109, reflecting consistency in data acquisition. These findings suggest that the CuO NPs exhibit sufficient colloidal stability, making them suitable for further incorporation into biopolymer-based wound dressing materials.

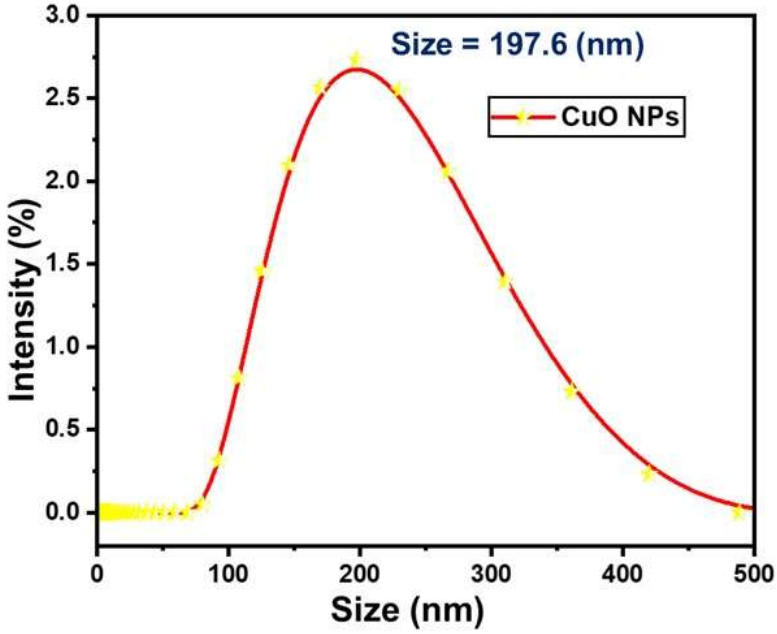

Fig.6. DLS particles size analysis of CuO NPs

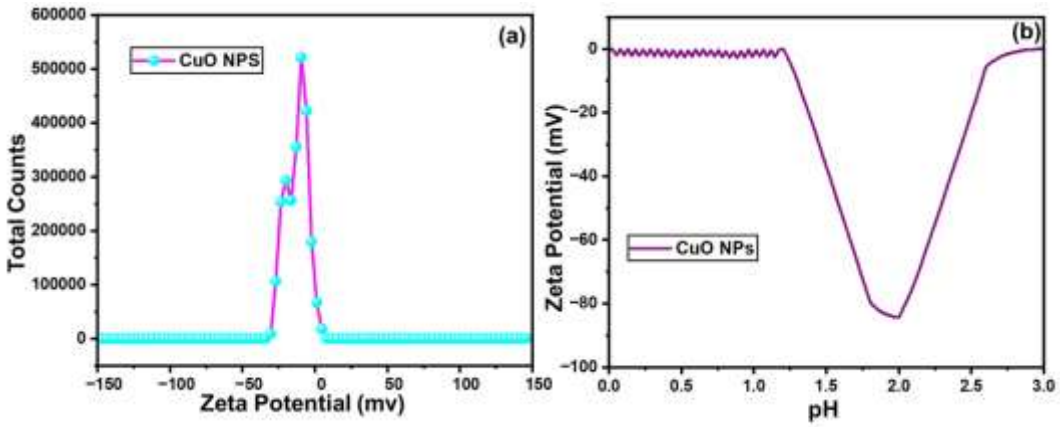

Fig.7. Zeta-potential analysis of CuO NPs

3.7. Wound healing (scratch) assay

After 48 hours of treatment, the wound healing assay (Fig. 8) demonstrated significant differences in the migratory behavior of HaCaT keratinocyte cells when exposed to algal extract, CuO NPs, and starch/PVA/CuO-NPs nanoscaffolds at varying concentrations (6.25–100 µg/mL). The untreated control exhibited a baseline migration rate, while all test samples enhanced wound closure in a concentration-dependent manner.

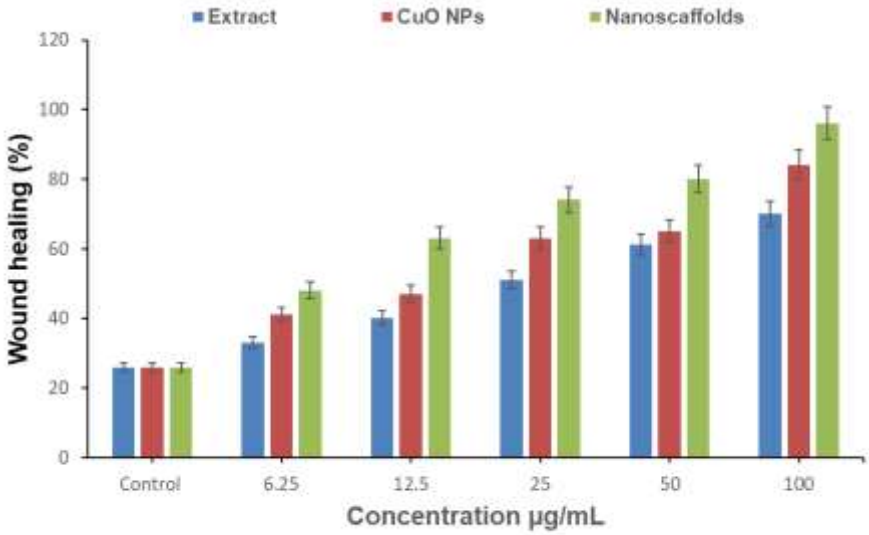

Fig. 8. Wound healing activity analysis of algal extract, CuO-NPs and starch/PVA/CuO-NPs nanoscaffolds

Algal Extract: The algal extract promoted wound closure, with migration rates increasing from 33.14% at 6.25 µg/mL to 70.14% at 100 µg/mL. This suggests that bioactive compounds in the extract stimulated keratinocyte migration, though its efficacy was moderate compared to the other treatments.

CuO NPs: CuO NPs exhibited stronger pro-migratory effects, with wound closure rates rising from 41.14% at 6.25 µg/mL to 84.14% at 100 µg/mL. The nanoparticles significantly accelerated cell migration, likely due to their role in enhancing cellular signaling pathways involved in wound repair.

Starch/PVA/CuO-NPs Nanoscaffolds: The nanoscaffolds displayed the most pronounced wound healing activity, achieving 48.14% closure at 6.25 µg/mL and 96.14% at 100 µg/mL. Their superior performance may be attributed to the combined effects of the biocompatible scaffold matrix and the embedded CuO NPs, which collectively support cell adhesion, proliferation, and migration.

All test samples enhanced wound healing compared to the control, with the nanoscaffolds showing the highest efficacy. The results highlight the potential of these materials, particularly the starch/PVA/CuO-NPs nanoscaffolds, as promising candidates for wound healing applications. Further studies could explore their mechanisms of action and *in vivo* performance.

4. DISCUSSION

The wound healing potential of starch/PVA electrospun nanoscaffolds integrated with biogenically synthesized CuO NPs derived from *S. muticum* was systematically assessed through multiple analytical and biological techniques. The study employed a comprehensive suite of characterization tools to confirm nanoparticle synthesis,

successful incorporation into polymer matrices, and biological efficacy using an *in vitro* scratch assay. Each analytical technique contributed valuable insights into the scaffold's physicochemical properties and its capability to enhance cellular responses associated with wound healing.

The UV–Visible spectroscopic analysis provided a foundational confirmation of nanoparticle formation. The *S. muticum* extract showed broad absorption due to its diverse phytochemical content, likely polyphenols and flavonoids. Upon reduction of copper salts through the ultrasonic-assisted green synthesis method, a distinct SPR peak emerged at 270 nm, indicating the presence of CuO NPs. The peak absorbance value of 0.4776 strongly supported the formation of stable nanoscale CuO structures. The optimized instrumental conditions ensured precise spectral resolution, and this transition from phytochemical-rich extract to nanomaterial is essential for demonstrating the success of green synthesis approaches. These findings confirmed the transformation of metal precursors into well-defined CuO NPs via eco-friendly processes [48-53].

FTIR spectral analysis further validated the integration of CuO NPs into the starch/PVA matrix. The presence of characteristic O–H and C–H stretching vibrations, along with aldehydic carbonyl bands in the CuO spectrum, indicated functional groups derived from the algal extract were involved in reduction and capping. In the nanoscaffold, peaks at 1500 cm^{-1} and 840 cm^{-1} denoted the presence of carbonyl and glycosidic groups, respectively, suggesting the maintenance of essential polymer functionalities. Notably, bands below 1000 cm^{-1} confirmed the presence of Cu–O bonds, verifying successful embedding of the nanoparticles. This retention of functional groups implies that the structural and chemical integrity of the scaffold is preserved post-incorporation, which is critical for biocompatibility and sustained activity in biomedical environments [54-59].

XRD analysis demonstrated the crystalline nature of the biosynthesized CuO NPs and their effect on the scaffold's structure. The nanoparticles exhibited sharp peaks consistent with the monoclinic crystalline phase of CuO, corroborated by standard JCPDS data. In contrast, the starch/PVA scaffold, typically semicrystalline, showed additional reflections upon incorporation of CuO NPs, indicating a degree of structural reorganization. The calculated interplanar distances for the CuO NPs (2.73 Å) and scaffold (4.60 Å) supported the idea of homogeneous nanoparticle dispersion, which is vital for ensuring uniform therapeutic response throughout the scaffold surface [60-65].

SEM revealed the morphological attributes of both nanoparticles and scaffolds. The CuO NPs appeared as clusters with varied shapes, indicating moderate polydispersity. The electrospun starch/PVA nanofibers exhibited smooth, interconnected fibers with uniform porosity and minimal bead formation. Importantly, CuO NPs were well-integrated within the scaffold matrix, uniformly distributed across the fiber surfaces. This nanostructured architecture is advantageous for facilitating nutrient transport, cell infiltration, and gas exchange—key parameters for effective wound healing [66-71].

TGA established the thermal stability of the composite material. A three-phase decomposition pattern was observed, beginning with water evaporation, followed by polymer degradation, and concluding with stable residue retention. The retention of approximately 51.9% mass post-heating confirmed the presence of thermally stable CuO NPs and possibly crosslinked polymeric chains. This enhanced stability supports the scaffold's application in thermally dynamic environments such as skin wounds, where stability is necessary for prolonged action [72-74].

Zeta potential and DLS measurements provided insights into the colloidal stability and particle size distribution of the synthesized CuO NPs. The average particle size was 92.1 nm with a polydispersity index of 0.8444, indicating moderate uniformity. The zeta potential of −12.62 mV revealed moderate surface charge stability, sufficient to prevent aggregation in solution. These findings support the idea that the CuO NPs are appropriately stable for biological applications, including their incorporation into polymer scaffolds for controlled therapeutic release [75-78].

The most significant aspect of the study was the wound healing assay, which evaluated the biological efficacy of the various treatments using HaCaT keratinocyte cells. After 48 hours, a concentration-dependent response was observed across all treatment groups. The *S. muticum* extract alone facilitated moderate cell migration, attributed to its natural bioactive compounds. CuO NPs, known for their antimicrobial and regenerative properties, showed enhanced wound closure, suggesting their direct involvement in promoting keratinocyte migration and proliferation. The highest wound healing potential was recorded with the starch/PVA/CuO nanoscaffolds. The closure rate reached 96.14% at 100 µg/mL, indicating a synergistic effect between the biocompatible polymer matrix and the embedded CuO NPs. This combination likely offers a supportive environment for cell adhesion and directional migration, while simultaneously delivering therapeutic ions that stimulate healing processes. The porous, fibrous structure of the scaffold mimics the extracellular matrix (ECM), further enhancing its interaction with skin cells and facilitating rapid wound closure [79].

The integration of CuO NPs synthesized from *S. muticum* into starch/PVA electrospun nanoscaffolds presents a promising approach for wound healing applications. The detailed physicochemical characterizations confirmed successful nanoparticle formation and embedding, while the biological assays demonstrated superior healing performance. The combined properties of antimicrobial activity, scaffold support, and bioactive ion release establish these nanocomposites as viable candidates for next-generation wound dressings. Future studies should include *in vivo* validations and long-term biocompatibility assessments to fully realize their clinical potential.

5. CONCLUSION

This study successfully demonstrated the fabrication and therapeutic potential of starch/PVA electrospun nanoscaffolds loaded with biogenic CuO NPs synthesized from *S. muticum* extract for enhanced wound healing. Comprehensive characterization using UV-Vis, FTIR, XRD, SEM, and TGA confirmed the successful formation of crystalline CuO NPs with optimal stability and their uniform integration into the nanofibrous scaffold. The *in vitro* scratch assay revealed that the nanoscaffold significantly accelerated HaCaT keratinocyte migration, achieving 96.14% wound closure at 100 µg/mL—outperforming both algal extract and CuO NPs alone. This superior efficacy can be attributed to the synergistic combination of the scaffold's biomimetic architecture, which promotes cell adhesion, and the bioactive CuO NPs, which enhance cellular repair mechanisms. The results underscore the potential of these nanocomposite scaffolds as advanced wound dressings, offering a biocompatible, sustainable, and highly effective alternative to conventional treatments. Future studies should focus on *in vivo* validation and mechanistic insights to further optimize their clinical applicability.

Ethical Declaration: Not Applicable

Data Availability Statement: The full dataset of physiochemical characterization associated with this work is published in Mendeley Data [Dataset] Bioactive nanostructured platforms: Physicochemical assessment of starch scaffolds hybridized with *Sargassum muticum*-copper oxide nanoparticles (DOI: 10.17632/jrs2y2hp7v.2). Disclosure: The material characterization data and figures (e.g., UV, SEM, FTIR, XRD, TGA, Zeta Potential and particle sizer) presented here were generated from a common dataset and are being reused across multiple related studies on nanomaterials. All biological analyses and conclusions are original to each manuscript.

Conflicts of Interest: The authors declare no conflicts of interest.

REFERENCES

[1] Huang Y, Guo H, Liu Y, Jin W, Palanisamy CP, Pei J, Oz F, El-Aty AMA. Effects of Natural Polysaccharides on the Gut Microbiota Related to Human Metabolic Health. Molecular Nutrition & Food Research. 2025; 69:e202400792.

[2] Poornima K, Meenakshi K.C, Manikandan V.R, Shankari G, Prabhu D, Rathi M.A, Palanisamy CP, Balaji R, Gopalakrishnan V.K. Exploring the anticancer potential of Jerantinine A from *Tabernaemontana coronaria* against prostate, breast, and ovarian cancers: A computational approach. *Journal of Complementary and Integrative Medicine*, 2025 22(2): 363–372.

[3] Palanisamy CP, Poompradub S, Sansanaphongpricha K, Jayaraman S, Subramani K. Faridah Sonsudin gGreen synthesis of Nigella sativa-mediated silver nanoparticles for enhanced antibacterial activity and wound healing: Mechanistic insights and biomedical applications. Environmental Nanotechnology, Monitoring & Management. 2025; 24: 101085.

[4] Surendran N, Raju MV, Chandrasekaran MK, Ahalliya RM, Palanisamy CP, Chandrasekaran G, Kanniappan GV. Physicochemical characterization of starch from Maranta arundinacea L.(arrowroot) rhizomes and its inhibition of COX-2: In vivo validation. Bioactive Carbohydrates and Dietary Fibre. 2025; 33: 100465.

[5] Kannappan P, Chandrasekaran MK, Raju MV, Gopalakrishnan S, Dhamodharan P, Ahalliya RM, Palanisamy CP, Raju B, Kanniappan GV. Exploring the anticancer potential of Jerantinine A from Tabernaemontana coronaria against prostate, breast, and ovarian cancers: a computational approach. Journal of Complementary and Integrative Medicine. 2025; 22(02): 363-372.

[6] Pei J, Kumarasamy RV, Jayaraman S, Kanniappan GV, Long Q, Palanisamy CP. Quercetin-functionalized nanomaterials: Innovative therapeutic avenues for Alzheimer's disease management. Ageing Research Reviews. 2025; 104: 102665.

[7] Jayaraman S, Prasad M, Natarajan SR, Krishnamoorthy R, Alshuniaber MA, Gatasheh MK, Veeraraghavan VP, Rajagopal P, Palanisamy CP. Molecular mechanisms underlying the effects of beta-sitosterol on TGF-β1/Nrf2/SIRT1/p53-mediated signaling in the kidney of a high-fat diet and sucrose-induced type-2 diabetic rat. Chemico-Biological Interactions. 2025; 411: 111443.

[8] Huang Y, Guo H, Liu Y, Jin W, Palanisamy CP, Pei J, Oz F, El-Aty AMA. Effects of Natural Polysaccharides on the Gut Microbiota Related to Human Metabolic Health. Molecular Nutrition & Food Research. 2025; e202400792.

[9] Prabhakaran P, Palanisamy CP, Shanmugam A, Damodharan P, Swaminathan H, Devaraj D, Ahalliya RM, Kanniappan GV. Isolation, structural characterization, and molecular docking studies on the bioactive compound from n-Hexane extract of Emilia sonchifolia (L.) DC against the pancreatic cancer target Aurora 2 Kinase. Journal of Complementary and Integrative Medicine. 2024; 22(1): 0290.

[10] Jiang H, Kumarasamy RV, Pei J, Raju K, Kanniappan GV, Palanisamy CP. Integrating engineered nanomaterials with extracellular vesicles: Advancing targeted drug delivery and biomedical applications. Frontiers in Nanotechnology. 2024; 6: 1513683.

[11] Guo H, Liu Y, Wan T, Song D, Palanisamy CP, Geng J, Pei J, Özmen S, El-Aty AMA. Toward personalized cancer management: Role of precision nutrition–diet interventions. Journal of Functional Foods. 2024; 123: 106584.

[12] Natarajan SR, Krishnamoorthy R, Alshuniaber MA, Al-Anazi KM, Farah MA, Rajagopal P, Palanisamy CP, Veeraraghavan VP, Jayaraman S. Identification of FOXM1 as a novel protein biomarker and therapeutic target for colorectal cancer progression: Evidence from immune infiltration and bioinformatic analyses. International Journal of Biological Macromolecules. 282 (Part 4): 137201.
[13] Rajendran MS, Jayaraman S, Khan JM, Jasmine S, Prabhakaran RK, Raju MV, Chandrasekaran MK, Ahalliya RM, Kannappan P, Palanisamy CP, Kanniappan GV. Investigating the colon toxicity and carcinogenic role of monosodium glutamate compared with Dimethylhydrazine in male Wistar rats: Exploring the link to childhood colon cancer risk. Journal of King Saud University - Science. 2024; 36(11): 103507.
[14] Kumarasamy RV, Natarajan P, Umapathy VR, Roy JR, Rab SO, Saeed M, Panagal M, Mironescu M, Srinivasan GP, Palanisamy CP. Clinical Applications and Therapeutic Potentials of Advanced Nanoparticles: A Comprehensive Review on Completed Human Clinical Trials. Frontiers in Nanotechnology. 2024; 6:1479993.
[15] Jin W, Pei JJ, Roy JR, Jayaraman S, Ahalliya RM, Kanniappan GV, Mironescu M, Palanisamy CP. Comprehensive review on single-cell RNA sequencing: A new frontier in Alzheimer's disease research. Ageing Research Reviews. 2024; 274: 102454.
[16] Pei J, Palanisamy CP, Jayaraman S, Natarajan PM, Umapathy VR, Roy JR, Panagal M, Jayaraman S. Curcumin-loaded polymeric nanomaterials as a novel therapeutic strategy for Alzheimer's disease: A comprehensive review. Ageing Research Reviews. 2024; 99: 102393.
[17] Pei J, Palanisamy CP, Jayaraman S, Natarajan PM, Umapathy VR, Roy JR, Thalamati D, Ahalliya RM, Kanniappan GV, Mironescu M. A comprehensive review on starch-based Sustainable Edible Films Loaded with Bioactive Components for Food Packaging. International Journal of Biological macromolecules. 2024; 274 (Part-1): 133332.
[18] Palanisamy CP, poompradub S, Sansanaphongpricha K, Subramani K, Sonsudin F. Increased expression levels of PDGF and VEGF magnify the wound healing potential facilitated by biogenic synthesis of silver nanoparticles. Nano-Structures & Nano-Objects. 2024; 39: 101236.
[19] Pei J, Palanisamy CP, Jayaraman S, Natarajan PM, Umapathy VR, Roy JR, Thalamati D, Ahalliya RM, Kanniappan GV, Mironescu M. Proteomics Profiling of Extracellular Vesicle for Identification of Potential Biomarkers in Alzheimer's Disease: A Comprehensive Review. Ageing Research Reviews. 2024; 99: 102359.
[20] Xi J, Wang T, Xian P, Liu X, Du M, Yang H, Palanisamy CP, Lin W, Long Q. Proteomic insights uncover enhanced neurotherapeutic potential in conditioned mesenchymal stem cell-derived extracellular vesicles. Extracellular Vesicle. 2024; 3: 100037.
[21] Pei J, Natarajan PM, Umapathy VR, Swamikannu B, Sivaraman NM, Krishnasamy L, Palanisamy CP. Advancements in the synthesis and functionalization of zinc oxide-based nanomaterials for enhanced oral cancer therapy. Molecules. 2024; 29(11): 2706.
[22] Gatasheh MK, Natarajan SR, Krishnamoorthy R, Alsulami TS, Rajagopal P, Palanisamy CP, Veeraraghavan VP, Jayaraman S. Molecular analysis to identify novel potential biomarkers as drug targets in colorectal cancer therapy: an integrated bioinformatics analysis. Molecular and Cellular Oncology. 2024; 11(1): 2326699.
[23] Pei J, Yan Y, Jayaraman S, Rajagopal P, Natarajan PM, Umapathy VR, Gopathy S, Roy JR, Sadagopan CS, Thalamati D, Palanisamy CP, Mironescu M. A review on advancements in the application of starch-based nanomaterials in biomedicine: Precision drug delivery and cancer therapy. International Journal of Biological Macromolecules. 2024; 130746.
[24] Pei JJ, Yan Y, Palanisamy CP, Jayaraman S, Natarajan PM, Umapathy VR, Gopathy S, Roy JR, Sadagopan JC, Thalamati D, Mironescu M. Materials-based drug delivery approaches: Recent advances and future perspectives. Green Processing and Synthesis. 2024; 13: 20230094.
[25] Pei JJ, Deng W, Liu Y, Guo Y, Chen J, Abdu H, Khan MR, Palanisamy CP, El-Aty AM. A Comprehensive Review of Cornus officinalis: Health Benefits, Phytochemistry, and Pharmacological Effects for Functional Drug and Food Development. Frontiers in Nutrition. 2023; 10: 1309963.
[26] Alugoju P, Palanisamy CP, Anthikapalli NVA, Jayaraman S, Prasanskulab A, Chuchawankul S, Dyavaiah M, Tencomnao T. Exploring the anti-aging potential of natural products and plant extracts in budding yeast Saccharomyces cerevisiae: A review. F1000Research. 2023; 12: 1265.
[27] Lavanya M, Krishnamoorthy R, Alshuniaber MA, Manoharadas S, Palanisamy CP, Veeraraghavan VP, Jayaraman S, Rajagopal P, Padmini R. Formulation, characterization and evaluation of gelatin-syringic acid/zinc oxide nanocomposite for its effective anticancer, antioxidant and anti-inflammatory activities. Journal of King Saud University-Science. 2023; 35: 102909.
[28] Palanisamy CP, Poompradub S, Sansanaphongpricha K, Jayaraman S, Subramani K, Sonsudin F. Biosynthesis of silver nanoparticles (AgNPs) using ethanolic extract of Nigella sativa (L.) seeds promotes wound healing via PDGF and VEGF signalling pathways activation. Biocatalysis and Agricultural Biotechnology. 2023; 54: 102970.
[29] Prasad M, Jayaraman S, Natarajan SR, Veeraraghavan VP, Krishnamoorthy R, Gatasheh MK, Palanisamy CP, Elrobh M. Piperine modulates IR/Akt/GLUT4 pathways to mitigate insulin resistance: Evidence from animal and computational studies. International Journal of Biological Macromolecules. 2023; 253: 127242.
[30] Palanisamy CP, Pei JJ, Phaniendra A, Venkata AAN, Jayaraman S, Veeraragahavan VP, Sridevi G, Roy JR, Janaki CS, Thalamati D, Mironescu M, Luo Q, Chai Y, Long Q. New Strategy of Neurodegenerative Disease

Treatment with Extracellular Vesicles (EVs) Derived from Mesenchymal Stem Cells (MSCs). *Theranostics*. 2023; 13(12):4138-4165. doi:10.7150/thno.83066.
[31] Palanisamy CP, Phaniendra A, Jayaraman S, Poompradub S. *Nigella sativa* L. seed extracts promotes wound healing progress by activating VEGF and PDGF signalling pathways: *An in vitro* and *in silico* study. *F1000 Research*. 2023; 12: 436.
[32] Pei JJ, Palanisamy CP, Phaniendra A, Venkata AAN, Natarajan PM, Umapathy VR, Swamikannu B, Jayaraman S, Rajagopal P, Poompradub S. A comprehensive review on bio-based materials for chronic diabetic wounds. *Molecules*. 2022; 28(2), 604.
[33] Palanisamy CP, Cui B, Zhang H, Gunasekaran VP, Ariyo A, Jayaraman S, Veeraraghavan V, Rajagopal P. A critical review on starch-based electrospun nanofibrous scaffolds for wound healing application. International Journal of Biological Macromolecules. 2022; 222 (Part: B): 1852-1860.
[34] Monisha P, Selvaraj J, Mohamed AE, Mohamed E, Mosaab AEA, Vishnu PV, Srinivasan V, Vidhya RU, Shazia FJH, Kalaiselvi K, Durairaj S, Palanisamy CP, Surapaneni K M, Ponnulakshmi R. A Comprehensive review on therapeutic perspectives of phytosterols in insulin resistance: A mechanistic approach. Molecules. 2022; 27(5): 1595.
[35] Natarajan PM, Umapathy VR, Murali A, Swamikannu B. (2022). Computational Simulations of Identified marine-derived Natural Bioactive Compounds As Potential Inhibitors of Oral Cancer. Future Science OA. 2022; 8(3).
[36] Natarajan PM, Umapathy VR. Role of transcriptomics in the study of oral cancer. Frontiers in Oral Health. 2025; 6:1524364.
[37] Vidhyarekha U, Natarajan PM, Bhuminathan S, Sabarinathan J, Suba R, Vijayalakshmi P. Role of artificial intelligence in Oral Cancer. Advances in Public Health. 2024. 2024: 3664408.
[38] Ganesan A, Kumar NG, Natarajan PM, Gauthaman J. Automated classification of elongated styloid processes using deep learning models-an artificial intelligence diagnostics. Frontiers in Oral Health. 2025; 5: 1424840.
[39] Umapathy VR, Natarajan PM, Swamikannu B. Regenerative Strategies in Dentistry: Harnessing Stem Cells, Biomaterials and Bioactive Materials for Tissue Repair. Biomolecules. 2025; 15: 546.
[40] Natarajan PM. Dental Bioinformnatics-Current Scope and Future perspectives. Research Journal of Pharmacy and Technology. 2022;15(5):2351-6.
[41] Ganesan A, Kumar NG, Natarajan PM. Solanum trilobatum leaf extract-derived silver nanoparticles downregulate the PI3K/AKT/mTOR signaling pathway and attenuate oral squamous cell carcinoma cell proliferation. Journal of Herbmed Pharmacology. 2024; 13(2): 300-307.
[42] Perumal MKK, Renuka RR, Subbiah SK, Natarajan PM. Artificial intelligence-driven clinical decision support systems for early detection and precision therapy in oral cancer: a mini review. Frontiers in Oral Health. 2025; 6: 1592428.
[43] Ramesh E, Ganesan A, Lakshmi KC, Natarajan PM. Artificial intelligence-based diagnosis of oral leukoplakia using deep convolutional neural networks Xception and MobileNet-v2. Frontiers in Oral Health. 2025; 6: 1414524.
[44] Ganesan A, Kumar NG, Natarajan PM. Anticancer activity of silver nanoparticles synthesized from aqueous leaf extract of Solanum trilobatum (Purple fruit pea eggplant) on human oral cancer cells. Journal of Herbmed Pharmacololgy. 2024; 13(2): 260-268.
[45] Pei JJ, Perumal NC, Meng P, Long Q, Palanisamy CP. AI-assisted FTIR spectroscopic profiling of exosomes: Emerging frontiers in early detection of Alzheimer's disease. Ageing Research Reviews. 2026; 103311.
[46] Raja FSD, Abraham L, Rangasamy K, Saikia K, Rathankumar AK, Mironescu M, Mironescu I, Palanisamy CP, Kanniappan GV. Next-Generation Microbiome Therapeutics: Psychobiotics and Fecal Microbiota Transplants (FMT) for Mental Health Treatment. Frontiers in Cellular and Infection Microbiology. 2026; 16: 1719357.
[47] Subramani K, Srinivasan S, Shanmugam P, Palanisamy CP, Sonsudin F, Poompradub S. Sustainable phytochemical mediated-ZnO nanoparticles derived from Crescentia cujete for toxicological evaluation and multifunctional environmental applications. Environmental Nanotechnology, Monitoring & Management. 2026; 26: 101180.
[48] Kunamalla RP, Panagal M, Palanisamy CP. Green-engineered multiscale starch/PVA nanofibrous scaffolds embedded with CuO nanoparticles from Sargassum ilicifolium for potent antimicrobial performance. Genetics and Molecular Research. 2026; 25(13s): 1-9.
[49] Dharmaprakash S, Gunasekaran VP, Sivaramakrishnan R, Kanniappan GV, Jayaraman S, Mironescu M, Rajabathar JR, Mironescu ID, Palanisamy CP. Marine macroalgae-mediated ultrasonic-assisted green synthesis of CuO nanoparticles embedded in starch/PVA electrospun nanoscaffolds for in vitro α-amylase and α-glucosidase inhibitory activity. Scientific Reports. 2026; 16: 26243.
[50] Surendran N, Chandrasekaran G, Raju MV, Chandrasekaran MK, Ahalliya RM, Palanisamy CP, Kanniappan GV, Arcot R, Alharbi NS, Thiruvengadam M. Anti-inflammatory potential of ethanolic extract of Maranta arundinacea L.: Insights from COX-2 modulation and oxidative stress analysis. South African Journal of Botany. 2026; 195: 142-151.

[51] Pei J, Senthilkumar MV, Hessini K, Subramaniyam S, Sivaramakrishnan R, Kanniappan GV, Jayaraman S, Palanisamy CP. Green fabrication of starch/PVA/CuO nanoscaffolds using marine macroalgae extract for enhanced anti-inflammatory activity. Sustainable Chemistry and Pharmacy. 2026; 51: 102397.
[52] Balasubramanian V, Loganathan L, Muthuswamy K, Viswanathan TM, Raju MV, Chandrasekaran MK, Ahalliya RM, Poorasamy J, Palanisamy CP, Dominic S, Kanniappan GV. Anticancer therapeutic efficacy of PEGylated β-galactosidase from Aspergillus terreus in DMBA-induced breast cancer: Toxicological, molecular and histopathological evaluation in Wistar rats. International Journal of Biological Macromolecules. 2026; 360: 151856.
[53] Jayaraman S, Eswaran A, Rajagopal P, Palanisamy CP, Veerakumar P, Veeraraghavan VP, Sirasanagandla SR. Neuroendocrine-associated epigenetic factors in cellular senescence: mechanisms and therapeutic implications. Biogerontology. 2026; 27(2): 64.
[54] Ponnusamy B, Rajagopal P, Palanisamy CP, Veeraraghavan VP, Jayaraman S. Mechanistic Exploration of the anticancer activity of Justicia adhatoda Plant Leaf Ethanolic Extract against Colon Cancer Cells: An in silico and in vitro Approach. Asian Pacific Journal of Cancer Prevention. 2026; 27(3): 1069-1080.
[55] Pei J, Saran VS, Sivaramakrishnan R, Kanniappan GV, Pandurangan V, Jayaraman S, Dhayalan VK, Mironescu M, Mironescu ID, Palanisamy CP. Ultrasonic-assisted, Sargassum ilicifolium (brown marine macroalgae)-mediated biogenic synthesis of CuO nanoparticles incorporated in starch/PVA electrospun nanoscaffolds: In vitro safety and antioxidant efficacy assessment. Bioorganic Chemistry. 2026; 173: 109679.
[56] Raj MAPA, Subramaniyam S, Kanniappan GV, Jayaraman S, Palanisamy CP. Sustainable fabrication of starch/PVA/CuO electrospun nanoscaffolds from Turbinaria ornata (marine macroalgae) extract: Physicochemical characterization and antidiabetic evaluation. Kuwait Journal of Science. 2026; 53(2): 100545.
[57] Pei J, Ganesh NS, Subramaniyam S, Sivaramakrishnan R, Kanniappan GV, Jayaraman S, Palanisamy CP. Sustainable fabrication of starch/PVA/CuO electrospun nanoscaffolds from Padina tetrastromatica (Brown macroalgae) extract: Physicochemical characterization and antidiabetic assessment. Sustainable Chemistry One World. 2026; 9: 100195.
[58] Sakthiraj A, Sivaramakrishnan R, Subramaniyam S, Kanniappan GV, Pandurangan V, Jayaraman S, Dhayalan VK, Mironescu M, Mironescu ID, Palanisamy CP. Starch/PVA electrospun nanoscaffolds loaded with ultrasonic-assisted green-synthesis of CuO nanoparticles from marine macroalgae (Gracilaria corticata) extract: Cytotoxicity and antioxidant analysis. Chemical Physics Impact. 2026; 12: 101018.
[59] Raju M, Chandrasekaran MK, Loganathan L, Ahalliya RM, Mironescu M, Mironescu ID, Palanisamy CP, Kanniappan GV. Lipid remodeling and ferroptosis in phosphatidylcholine-mediated tumor–stroma crosstalk. Frontiers in Molecular Biosciences. 2026; 13: 1742305.
[60] Kunamalla R, Panagal M, Palanisamy CP. Biogenic synthesis and fabrication of starch/PVA/CuO electrospun nanoscaffolds from Sargassum ilicifolium (brown marine macroalgae) extract for anticancer activity on HT-29 and MCF-7 cancer cells. Biocatalysis and Agricultural Biotechnology. 2026; 72: 103923.
[61] Pei J, Govindaraj H, Sivaramakrishnan R, Kanniappan GV, Pandurangan V, Dhayalan VK, Mironescu M, Mironescu ID, Jayaraman S, Palanisamy PC. Sustainable fabrication of biopolymer-based (starch/PVA) nanoscaffolds loaded with green-synthesized CuO nanoparticles from Sargassum wightii (marine macroalgae): Cytocompatibility and antioxidant activity. Biomaterials Advances. 2026; 182: 214660.
[62] Pei J, Perumal NC, Meng P, Long Q, Palanisamy CP. Extracellular vesicle-based biosensors for Alzheimer's disease: A new frontier in precision diagnostics. Ageing Research Reviews. 2026; 113: 102904.
[63] Shree P, Sivaramakrishnan R, Kanniappan GV, Pandurangan V, Jayaraman S, Dhayalan VK, Mironescu M, Mironescu ID, Palanisamy CP. Antioxidant and biocompatible CuO-starch/PVA nanoscaffolds via ultrasonic green synthesis using Turbinaria conoides (brown marine macroalgae). Medicine in Drug Discovery. 2025; 28: 100238.
[64] Gong J, Lin J, Guan T, Pei J, Palanisamy CP, El-AtyFrom AMA. selenium tolerance to nanoplastic antagonism: Comprehensive characterization of L. casei SNUT1 and its extracellular vesicle–nanoselenium complex. Food Bioscience. 2025; 74: 107749.
[65] Poochi SP, Sundarraj R, Raju MV, Chandrasekaran MK, Ahalliya RM, Palanisamy CP, Kanniappan GV, Kondapavuluri BK, Thiruvengadam M. Harnessing Nature: Computational and Experimental Insights Into *Ipomoea obscura* Metabolites for Bladder Cancer Therapy. Chemistry and Biodiversity. 2025; 0: e00909.
[66] Dugganaboyana GK, Kannankumar MKG, Shivaramakrishna S, Raju MV, Chandrasekaran MK, Ahalliya RM, Panneerselvam N, Palanisamy CP, Kanniappan GV. Phytochemical insights, antioxidant activity and therapeutic potential of Cassia senna against prostate cancer in Wistar albino rats. Discover Applied Sciences. 2025; 7:1206.
[67] Natarajan SR, Krishnamoorthy R, Alshuniaber MA, Gatasheh MK, Rajagopal P, Veeraraghavan VP, Palanisamy CP, Jayaraman S. KDM1A Facilitates Oncogenic Potential in Colorectal Cancer Progression Through the Activation of AXIN/GSK3β/β-Catenin Signaling Pathways: Evidence From Integrated Transcriptomics and In Vitro Studies. The Journal of Gene Medicine. 2025; 27(11): e70053.
[68] Guan T, Gong J, Lin J, Palanisamy CP, Jinjin Pei J, El-Aty AMA. Machine learning-driven multimodal optimization of selenium biotransformation and flavor profiling in fermented apple–Yacon functional beverages. Innovative Food Science & Emerging Technologies. 2025; 105: 104198.
[69] Natarajan SR, Krishnamoorthy R, Alshuniaber MA, Alsulami TS, Gatasheh MK, Rajagopal P, Palanisamy

CP, Govindan R, Veeraraghavan VP, Jayaraman S. ABCE1 facilitates tumour progression via aerobic glycolysis and inhibits cell death in human colorectal cancer cells through the p53 signalling pathway. Scientific Reports. 2025; 15: 24674.
[70] Natarajan PM, Swamikannu B, Sivaraman NM, Stylin AGSQ. Prevention of Oral Cancer: A Comprehensive Guide. Journal of Pharmacy and Bioallied Sciences. 2024; 16(5): S4239-S4241.
[71] Umapathy V, Dhanavel A, Kesavan R, Natarajan PM, Bhuminathan S, Vijayalakshmi P. Anticancer Potential of the Principal Constituent of Piper nigrum, Piperine: A Comprehensive Review. Cureus. 2024; 16(2): e54425.
[72] Umapathy VR, Swamikannu B, Natarajan PM, Devi R, Nandini MS, Vimalarani, Vijayalakshmi P. In Silico Molecular Docking of Ocimum sanctum Phytochemicals: Targeting Key Biomarkers in Oral Cancer. Journal of Pharmacy and Bioallied Sciences. 2024; 16(5): S4792-S4799.
[73] Natarajan PM, Bhuminathan S, Rajan R, Bindu K, Loganathan K, Veerakumar R. The Crucial Role of Smoking Cessation in Preventing Oral Cancer. Journal of Pharmacy and Bioallied Sciences. 2024; 16(5): S4245-S4247.
[74] Swamikannu B, Umapathy VR, Natarajan PM, Nandini MS, Stylin AGSQ, Vimalarani V, Rajinikanth S. Unlocking the Therapeutic Benefits of Artemisia Annua: A Comprehensive Overview of its Medicinal Properties. Journal of Pharmacy and Bioallied Sciences. 2024; 16(5): S4248-S4253.
[75] Natarajan PM. Computational Studies on Recent Congeners of Fluoroquinolones and Nitroimidazoles for Their Use in Periodontal Therapy. Journal of Pharmacy and Bioallied Sciences. 2024; 16(5): S4731-S4740.
[76] Yadalam PK, Arumuganainar D, Natarajan PM, Ardila CM. Artificial intelligence-powered prediction of AIM-2 inflammasome sequences using transformers and graph attention networks in periodontal inflammation. Scientific Reports. 2025; 15: 8733.
[77] Yadalam PK, Chatterjee S, Natarajan PM, Ardila CM. Comparison of light gradient boosting and logistic r egression for interactomic hub genes in Porphyromonas gingivalis and Fusobacterium nucleatum-induced perio dontitis with Alzheimer's disease. Frontiers in Oral Health. 2025; 6:1463458.
[78] Natarajan PM, Bhuminathan S, Leela B, Bindu K, Loganathan K, Ramachandran V. Smoking and its Role in Oral Cancer. Journal of Pharmacy and Bioallied Sciences 16(5): S4242-S4244.
[79] Yadalam PK, Natarajan PM, Ardila CM. Variational graph autoencoder for reconstructed transcriptomic data associated with NLRP3 mediated pyroptosis in periodontitis. Scientific Reports. 2025; 15: 1962.